

Exclusive photoproduction of B_c^\pm and bottomonia pairs

Sebastián Andrade, Marat Siddikov, Iván Schmidt

*Departamento de Física, Universidad Técnica Federico Santa María,
y Centro Científico - Tecnológico de Valparaíso, Casilla 110-V, Valparaíso, Chile*

In this paper we analyze the photoproduction of heavy quarkonia pairs which include b -quarks, such as $B_c^+ B_c^-$ -mesons or charmonium-bottomonium pairs. Compared to charmonia pair production, these channels get contributions only from some subsets of diagrams, and thus allow for a better theoretical understanding of different production mechanisms. In contrast to the production of hidden-flavor quarkonia, for the production of B_c -meson pairs there are no restrictions on internal quantum numbers in the suggested mechanisms. Using the Color Glass Condensate approach, we estimated numerically the production cross-sections in the kinematics of the forthcoming Electron-Proton collider and in the kinematics of ultraperipheral collisions at LHC. We found that the production of $J/\psi \eta_c$ and $B_c^+ B_c^-$ meson pairs are the most promising channels for studies of quarkonia pair production.

I. INTRODUCTION

Since the early days of QCD, heavy quarkonia have been used for the study of the gluonic field in high energy interactions. Due to their heavy masses, the heavy quarks, which constitute the quarkonia, might be described in a perturbative approach [1, 2]. Nowadays the heavy quarks processes are described in the so-called NRQCD framework, which allows to incorporate systematically various perturbative corrections [3–14]. The studies of quarkonia usually focus on charmonia, since they have significantly larger cross-sections. However, it is known that in the charm sector there are certain technical challenges, such as for example the “non-universality” of the long-distance matrix elements, which potentially might be due to sizable corrections to the heavy quark mass limit. In contrast, for quarkonia including bottom quarks it is expected that the heavy quark mass approximation is much more reliable, and thus the expected corrections should be much smaller. A special place in these studies occupy the B_c^\pm -mesons, which are made of a b - and c -quarks. As of now these states are poorly understood, and only two states are included in the Particle Data Group’s listings. In the case of different heavy flavors, the hadronic decays of these mesons are forbidden due to lack of phase space, which implies quite a large mean lifetime. For the same reason, they have completely different production mechanisms compared to the hidden-flavor states: the B_c^\pm might be produced hadronically only in hard subprocesses, which include both $b\bar{b}$ and $c\bar{c}$ quark pairs at the partonic level. Due to this fact, their production cross-sections are very small. Nevertheless, studies of B_c^\pm production are important for the confirmation of our current understanding of heavy quarkonia in general, as well as providing a potential gateway for the study of various exotic multi-quark states in their decay products.

The *exclusive* production of heavy quarkonia is one of the cleanest channels for their study. Most of the previous work on this topic focused on single quarkonia states, due to their largest cross-section. However, the production of multiple heavy quarkonia (e.g. heavy quarkonia pairs) has been a subject of theoretical attention almost since inception of QCD [15–18]. The interest in this channel has drastically increased recently due to the forthcoming launch of high-luminosity accelerator facilities and a recent discovery of all-heavy tetraquarks, which might be molecular states of quarkonia pairs [19–29]. Nowadays such processes might be studied both in ultraperipheral collisions at the LHC, as well as in electron-proton collisions at the forthcoming Electron Ion Collider (EIC) [30–33], the future Large Hadron electron Collider (LHeC) [34], and the Future Circular Collider (FCC-he) [35–37].

Most of the previous studies of exclusive double quarkonia production focused on the so-called two-photon mechanism, $\gamma\gamma \rightarrow M_1 M_2$, which gives the dominant contribution to the production of quarkonia pairs with the same C -parity [38–43]. Recently we suggested an alternative mechanism, which has significantly larger cross-section, although leads to the production of charmonia pairs with opposite C -parities. In this paper we plan to extend those studies and analyze in detail the production of quarkonia including b -quarks. For all-bottomonia pairs this study essentially repeats our previous analysis of the charmonia sector, yet eventually gives extremely small cross-sections. More interest present mixed charmonium-bottomonium pairs, such as for example $J/\psi - \eta_b$ or $\Upsilon - \eta_c$, as well as the production of $B_c^+ B_c^-$ meson pairs. The production of these states obtains contributions only from some of the diagrams which are relevant for the production of all-charm or all-bottom quarkonia. In the case of $B_c^+ B_c^-$ production, there are no restrictions on internal quantum numbers of the produced mesons, which presents an important advantage over the charmonia pairs. According to theoretical expectations, the production cross-sections in these channels are maximal in the near-threshold region, which is relevant for searches of different exotic states, like e.g. $b\bar{b}$ -containing tetraquarks [44].

Both in ultraperipheral collisions at LHC and in ep collisions at future colliders the dominant contribution stems

from quasi-real photons with small virtuality $Q^2 \approx 0$. At central rapidities it is expected that the produced quarkonia will carry a just small fraction of the colliding hadron momenta, $x_i \ll 1$. In this kinematics the saturation effects should play an important role in the dynamics of partons, and thus should be properly accounted for in the theoretical models of interaction. In what follows we'll use the the color dipole framework, also known as Color Glass Condensate or CGC framework [45–53], which naturally incorporates the saturation effects and provides a phenomenologically successful description of both hadron-hadron and lepton-hadron collisions [54–61].

The paper is structured as follows. Below in Section II we present the theoretical results for the exclusive photoproduction of heavy quarkonia pairs in the CGC approach. In Section III we present our numerical estimates for meson pairs which include at least one b or \bar{b} -quark, and analyze the dependence on quantum numbers of produced quarkonia. Finally, in Section IV we draw conclusions.

II. EXCLUSIVE PHOTOPRODUCTION OF MESON PAIRS

Nowadays, photoproduction processes might be studied both in electron-proton, proton-proton and proton-nuclear collisions in ultraperipheral kinematics. The corresponding cross-sections of these processes are related to photoproduction cross-section as

$$\frac{d\sigma_{ep \rightarrow eM_1M_2p}}{dQ^2 dy_1 d^2\mathbf{k}_1^\perp dy_2 d^2\mathbf{k}_2^\perp} \approx \frac{\alpha_{em}}{\pi Q^2} \left(1 - y + \frac{y^2}{2}\right) \frac{d\sigma_T(\gamma + p \rightarrow \gamma + p + M_1 + M_2)}{dy_1 d^2\mathbf{p}_1^\perp dy_2 d^2\mathbf{p}_2^\perp} \Big|_{\mathbf{p}_a^\perp \approx \mathbf{k}_a^\perp}, \quad (1)$$

$$\frac{d\sigma_{pA \rightarrow pAM_1M_2}}{dy_1 d^2\mathbf{k}_1^\perp dy_2 d^2\mathbf{k}_2^\perp} = \int dn_\gamma(\omega \equiv E_\gamma, \mathbf{q}_\perp) \frac{d\sigma_T(\gamma + p \rightarrow \gamma + p + M_1 + M_2)}{dy_1 d^2\mathbf{p}_1^\perp dy_2 d^2\mathbf{p}_2^\perp} \Big|_{\mathbf{p}_a^\perp \approx \mathbf{k}_a^\perp - \mathbf{q}^\perp} \quad (2)$$

where in (1) we use standard DIS notation in which y is the inelasticity (fraction of electron energy which passes to the photon), and $(y_a, \mathbf{k}_a^\perp)$, with $a = 1, 2$, are the rapidities and transverse momenta of the produced quarkonia with respect to electron-proton or hadron-hadron collision axis. The expression $dn_\gamma(\omega \equiv E_\gamma, \mathbf{q}_\perp)$ in (2) is the spectral density of the flux of equivalent photons with energy E_γ and transverse momentum \mathbf{q}_\perp with respect to the nucleus, which was found explicitly in [62]. The momenta $\mathbf{p}_a^\perp = \mathbf{k}_a^\perp - \mathbf{q}_\perp$ are the transverse parts of the quarkonia momenta with respect to the produced photon. The nuclear form factors strongly suppress the transverse momenta \mathbf{q}_\perp larger than the inverse nuclear radius R_A^{-1} . For this reason the average values of \mathbf{q}_\perp are quite small, $\langle \mathbf{q}_\perp^2 \rangle \sim \langle Q^2 \rangle \sim \langle R_A^2 \rangle^{-1} \lesssim (0.2 \text{ GeV}/A^{1/3})^2$, and the p_\perp -dependence of the cross-sections in the left-hand side of (2) almost coincides with the p_\perp -dependence of the cross-section in the integrand in the right-hand side. The subscript letter T in the right-hand side of (1) reminds us that the dominant contribution comes from quasireal transversely polarized photons. The corresponding cross-section $d\sigma_T$ is related to the amplitude as

$$\frac{d\sigma_T}{dy_1 d|p_1^\perp|^2 dy_2 d|p_2^\perp|^2 d\phi} \approx \frac{1}{256\pi^4} |\mathcal{A}_{\gamma Tp \rightarrow M_1 M_2 p}|^2 \delta\left(\frac{p_1^+ + p_2^+}{q^+} - 1\right), \quad (3)$$

where $\mathcal{A}_{\gamma Tp \rightarrow M_1 M_2 p}$ is the amplitude of the exclusive process, induced by a transversely polarized photon, and ϕ is the angle between the vectors \mathbf{p}_1^\perp and \mathbf{p}_2^\perp in transverse plane. The variable q^+ is the light-cone momentum of the photon, and p_1^+, p_2^+ are the light-cone momenta of the produced quarkonia. As we will show below, it is possible to express them via quarkonia kinematic variables $(y_a, \mathbf{p}_a^\perp)$.

For further evaluations of the amplitude $\mathcal{A}_{\gamma Tp \rightarrow M_1 M_2 p}$ it is necessary to fix the reference frame and write out explicit light-cone momenta decompositions of the participating hadrons. In what follows we will use the notations: q for the photon momentum, P and P' for the momentum of the proton before and after the collision, and p_1, p_2 for the 4-momenta of produced heavy quarkonia. We will also use the notation Δ for the momentum transfer to the proton, $\Delta = P' - P$, and t for its square, $t \equiv \Delta^2$. The light-cone expansion of the above-mentioned momenta in the lab frame

is given by

$$q = (q^+, 0, \mathbf{0}_\perp), \quad q^+ \approx 2E_\gamma \quad (4)$$

$$P = \left(\frac{m_N^2}{2P^-}, P^-, \mathbf{0}_\perp \right), \quad P^- = E_p + \sqrt{E_p^2 - m_N^2} \approx 2E_p \quad (5)$$

$$P' \approx \left(\frac{m_N^2 + (\mathbf{p}_1^\perp + \mathbf{p}_2^\perp)^2}{2P^- - M_1^\perp e^{-y_1} + M_2^\perp e^{-y_2}}, P^- - \frac{M_1^\perp e^{-y_1} + M_2^\perp e^{-y_2}}{2}, -\mathbf{p}_1^\perp - \mathbf{p}_2^\perp \right), \quad (6)$$

$$p_a = \left(M_a^\perp e^{y_a}, \frac{M_a^\perp e^{-y_a}}{2}, \mathbf{p}_a^\perp \right), \quad a = 1, 2, \quad (7)$$

$$M_a^\perp \equiv \sqrt{M_a^2 + (\mathbf{p}_a^\perp)^2}, \quad (8)$$

where m_N is the mass of the nucleon, and M_1, M_2 are the masses of produced quarkonia. In the high-energy collider kinematics, when $q^+, P^- \gg \{Q, M_a, m_N, \sqrt{|t|}\}$, there is an approximate relation between the energy (component q^+) of the photon and the light-cone momenta of the produced quarkonia,

$$q^+ \approx 2E_\gamma \approx M_1^\perp e^{y_1} + M_2^\perp e^{y_2}, \quad (9)$$

which in essence reflects the fact that the change of the light-cone plus-component proton momentum, $(P')^+ - P^+$, is negligibly small, in agreement with the eikonal picture expectations. The relations (4-9) allow to express the quarkonia kinematic variables $(y_a, \mathbf{p}_a^\perp)$ in terms of conventional DIS variables, such as the Bjorken variable x_B or invariant energy $W = \sqrt{s_{\gamma p}}$. In what follows we will use these variables $(y_a, \mathbf{p}_a^\perp)$, since they allow to keep explicit an symmetry w.r.t. permutation of quarkonia, and are directly measurable in experiments. In terms of these variables, the invariant energy W of the γp collision and the invariant mass M_{12} of the produced heavy quarkonia pair are given by

$$W^2 \equiv s_{\gamma p} = (q + P)^2 = -Q^2 + m_N^2 + 2q \cdot P \approx -m_N^2 + P^- (M_1^\perp e^{y_1} + M_2^\perp e^{y_2}), \quad (10)$$

and

$$M_{12}^2 = (p_1 + p_2)^2 = M_1^2 + M_2^2 + 2(M_1^\perp M_2^\perp \cosh \Delta y - \mathbf{p}_1^\perp \cdot \mathbf{p}_2^\perp) \quad (11)$$

respectively. The photoproduction amplitude $\mathcal{A}_{\gamma T p \rightarrow M_1 M_2 p}$, which appears in (3), is the central quantity of interest for our study. Since the formation time of quarkonia is larger than the typical size of the proton, the amplitude of the process might be factorized and written as a convolution of the quarkonia wave functions with hard amplitudes which describe photoproduction of two quark-antiquark pairs in the gluonic field of the target. In what follows we will refer to the heavy quarks produced in such hard subprocess as “final state” quarks. The studies of exclusive production are usually performed in the kinematics of small momenta p_T , so we may expect that possible contributions of the color octet mechanisms [8, 9] are small and might be omitted. While there is no direct experimental check of this assumption, similar studies of *single* quarkonia photoproduction in exclusive processes [63–65] provide indirect evidence that this assumption might be quite reliable.

The amplitude of the double quarkonia photoproduction has been evaluated in [66] using the color dipole (Color Glass Condensate) approach [45, 47–53]. That evaluation was performed for the charm sector, focusing on the production of $J/\psi \eta_c$ pairs. In this paper we are going to extend those results for the case in which the final state quarkonia include b -quarks. For the production of mixed states, such as $J/\psi \eta_b$, $\Upsilon \eta_b$ and $B_c^+ B_c^-$ meson pairs, only some subsets of diagrams contribute to the total cross-section, thus providing the possibility to understand the relative contribution of different mechanisms.

In the color dipole approach the hard process is considered in the eikonal picture. Taking into account that the interactions of heavy quarks with the gluonic field of the target are suppressed by the strong coupling $\alpha_s(m_Q)$, all the leading order diagrams might be grouped into two main classes, shown schematically in Figure 1. In what follows we will call them “type- A ” and “type- B ” respectively, and take into account that the amplitude of the whole process might be written as an additive sum,

$$\mathcal{A}(y_1, \mathbf{p}_{T1}, y_2, \mathbf{p}_{T2}) = \mathcal{A}^{(A)}(y_1, \mathbf{p}_{T1}, y_2, \mathbf{p}_{T2}) + \mathcal{A}^{(B)}(y_1, \mathbf{p}_{T1}, y_2, \mathbf{p}_{T2}), \quad (12)$$

where $\mathcal{A}^{(A)}$ and $\mathcal{A}^{(B)}$ are the contributions of the respective classes. For the production of all-charm or all-bottom quarkonia pairs, both $\mathcal{A}^{(A)}$ and $\mathcal{A}^{(B)}$ give nonzero contribution. In this case, C -parity conservation indicates that the produced quarkonia must have opposite C -parities. For the production of mixed $B_c^+ B_c^-$ meson pairs, the amplitude

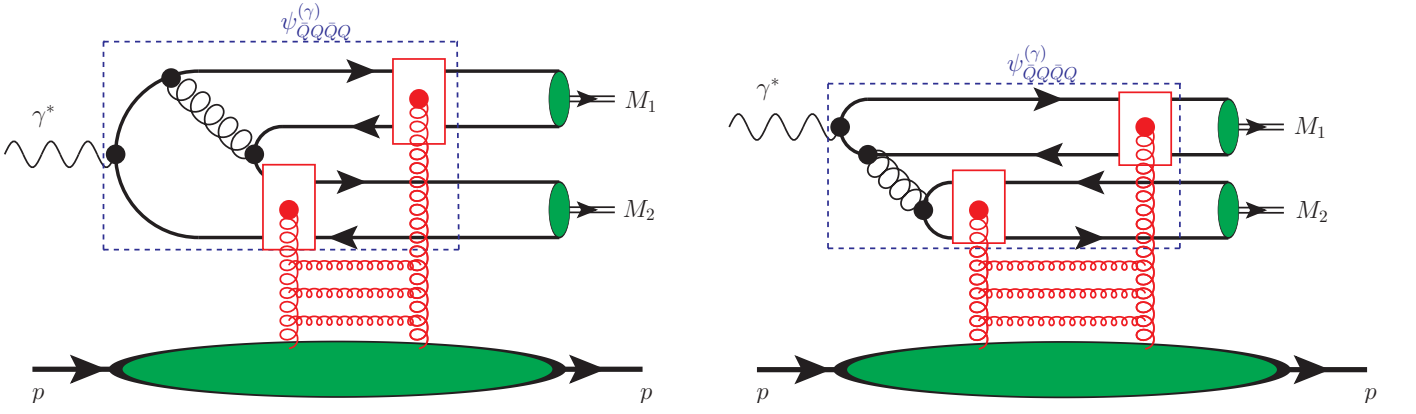


Figure 1. Main classes of diagrams which contribute in the leading order over $\alpha_s(m_Q)$ to exclusive photoproduction of quarkonia pairs (type-A and type-B diagrams). The eikonal interactions are shown schematically as exchanges of t -channel gluons, indicated by the red wavy lines. In both plots it is implied: (a) summation over all possible attachments of t -channel gluons to partons inside blue dashed rectangle in upper part of diagram (b) inclusion of diagrams with inverted direction of heavy quark lines (“charge conjugation”). In the right diagram the t -channel gluons must be connected to different quark loops in order to guarantee production of *color singlet* $Q\bar{Q}$ in final states. The blue dashed rectangle schematically shows part of the diagrams which (in absence of eikonal interactions) would contribute to the $Q\bar{Q}Q\bar{Q}$ -component of the photon wave function $\psi_{Q\bar{Q}Q\bar{Q}}^{(\gamma)}$.

$\mathcal{A}^{(B)} \equiv 0$, so only the type-A diagrams contribute. The C -parity conservation in this case does not impose any constraints on the produced B_c -quarkonia internal quantum numbers, although imposes constraints on the angular momentum L of the relative motion, which should take odd values. This constraint is relaxed if the produced B_c mesons have different spins, like *e.g.* $B_c^{*+}B_c^-$ or $B_c^+B_c^{*-}$, where B_c^{\pm} is the (so far undiscovered) vector state. Finally, for the production of charmonium-bottomonium pairs, such as $J/\psi\eta_b$ or $\Upsilon\eta_b$, we can see that $\mathcal{A}^{(A)} \equiv 0$, so the amplitude get contributions only of the type-B diagrams. Further analysis of the type-B diagrams allows to reach some conclusions about the relative size of mixed charmonium-bottomonium production cross-sections. Analysis of quantum numbers suggests that a vector particle ($J^P = 1^-$) might be produced only in the upper loop (with 3 gluon attachments to heavy quark line), whereas scalar particles might originate from the quark loop in lower part of the diagram. This observation allows to understand the behavior of the cross-section under permutation of charm and bottom flavors. Since in the heavy quark mass limit each gluon attachment is suppressed and the natural scale for heavy quark is its mass, we may immediately conclude that in channels with charmonium-bottomonium production, the states with vector bottomonia are suppressed significantly stronger than the states with vector charmonia. In the next section we will corroborate this expectation by explicit comparison of numerical predictions for $\Upsilon(1S)\eta_c$ and $J/\psi\eta_b$ production cross-sections.

In the eikonal picture the impact parameter of the parton is conserved during interaction with the target. The interaction of the colored dipole with the target might be described as a linear combination of the color singlet dipole scattering amplitudes, which are known from Deep Inelastic Scattering. For this reason, it becomes possible to rewrite both types of diagrams as a mere convolution of the four quark component of the photon wave function $\psi_{Q\bar{Q}Q\bar{Q}}^{(\gamma)}$ with final state quarkonia wave functions and a linear combination of color singlet dipole scattering amplitudes,

$$\begin{aligned}
\mathcal{A}^{(A)}(y_1, \mathbf{p}_{T1}, y_2, \mathbf{p}_{T2}) &= \prod_{i=1}^4 \left(\int d\alpha_i d^2\mathbf{x}_i \right) \delta \left(\sum_k \alpha_k - 1 \right) \mathcal{N}^{(A)}(\alpha_1, \mathbf{x}_1; \alpha_2, \mathbf{x}_2; \alpha_3, \mathbf{x}_3; \alpha_4, \mathbf{x}_4) \times \\
&\times \left[\Psi_{M_1}^\dagger(\alpha_{14}, \mathbf{r}_{14}) \Psi_{M_2}^\dagger(\alpha_{23}, \mathbf{r}_{23}) e^{i(\mathbf{p}_1^\perp \cdot \mathbf{b}_{14} + \mathbf{p}_2^\perp \cdot \mathbf{b}_{23})} \delta(y_1 - \mathcal{Y}_{14}) \delta(y_2 - \mathcal{Y}_{23}) \right. \\
&+ \left. \Psi_{M_1}^\dagger(\alpha_{23}, \mathbf{r}_{23}) \Psi_{M_2}^\dagger(\alpha_{14}, \mathbf{r}_{14}) e^{i(\mathbf{p}_1^\perp \cdot \mathbf{b}_{23} + \mathbf{p}_2^\perp \cdot \mathbf{b}_{14})} \delta(y_1 - \mathcal{Y}_{23}) \delta(y_2 - \mathcal{Y}_{14}) \right] \\
&\times \psi_{Q\bar{Q}Q\bar{Q}}^{(\gamma)}(\alpha_1, \mathbf{x}_1; \alpha_2, \mathbf{x}_2; \alpha_3, \mathbf{x}_3; \alpha_4, \mathbf{x}_4; q).
\end{aligned} \tag{13}$$

$$\begin{aligned}
\mathcal{A}^{(B)}(y_1, \mathbf{p}_{T1}, y_2, \mathbf{p}_{T2}) &= \prod_{i=1}^4 \left(\int d\alpha_i d^2 \mathbf{x}_i \right) \delta \left(\sum_k \alpha_k - 1 \right) \mathcal{N}^{(B)}(\alpha_1, \mathbf{x}_1; \alpha_2, \mathbf{x}_2; \alpha_3, \mathbf{x}_3; \alpha_4, \mathbf{x}_4) \times \\
&\times \left[\Psi_{M_1}^\dagger(\alpha_{12}, \mathbf{r}_{12}) \Psi_{M_2}^\dagger(\alpha_{34}, \mathbf{r}_{34}) e^{i(\mathbf{p}_1^\perp \cdot \mathbf{b}_{12} + \mathbf{p}_2^\perp \cdot \mathbf{b}_{34})} \delta(y_1 - \mathcal{Y}_{12}) \delta(y_2 - \mathcal{Y}_{34}) \right. \\
&+ \left. \Psi_{M_1}^\dagger(\alpha_{34}, \mathbf{r}_{34}) \Psi_{M_2}^\dagger(\alpha_{12}, \mathbf{r}_{12}) e^{i(\mathbf{p}_1^\perp \cdot \mathbf{b}_{34} + \mathbf{p}_2^\perp \cdot \mathbf{b}_{12})} \delta(y_1 - \mathcal{Y}_{34}) \delta(y_2 - \mathcal{Y}_{12}) \right] \\
&\times \psi_{\gamma^* \rightarrow \bar{Q}Q\bar{Q}Q}(\alpha_1, \mathbf{x}_1; \alpha_2, \mathbf{x}_2; \alpha_3, \mathbf{x}_3; \alpha_4, \mathbf{x}_4; q),
\end{aligned} \tag{14}$$

where in (13, 14) $\mathbf{r}_{ij} = \mathbf{x}_i - \mathbf{x}_j$ is the relative distance between partons i and j ; $\alpha_{ij} = \alpha_i / (\alpha_i + \alpha_j)$ is the light-cone fraction carried by the quark in the pair (ij) , and $\mathbf{b}_{ij} = (\alpha_i \mathbf{x}_i + \alpha_j \mathbf{x}_j) / (\alpha_i + \alpha_j)$ is the (transverse) position of the center of mass of (i, j) pair. The notations Ψ_{M_1}, Ψ_{M_2} are used for the wave functions of the final state quarkonia M_1 and M_2 (for a moment we disregard completely their spin indices), and $\psi_{\bar{Q}Q\bar{Q}Q}^{(\gamma)}(\{\alpha_i, \mathbf{x}_i\}; q)$ is the 4-quark light-cone wave function of the virtual photon γ^* which is given explicitly in Appendix A. The amplitudes $\mathcal{N}^{(A)}$ and $\mathcal{N}^{(B)}$ include resummation over all possible connections of t -channel gluons to quark lines and, as was shown in [66], can be rewritten as a linear superposition of the color singlet dipole amplitudes $N(x, \mathbf{r}_{ij}, \mathbf{b}_{ij})$

$$\begin{aligned}
\mathcal{N}^{(A)}(\alpha_1, \mathbf{x}_1; \alpha_2, \mathbf{x}_2; \alpha_3, \mathbf{x}_3; \alpha_4, \mathbf{x}_4) &= \\
&= \left\{ \frac{2 - N_c^2}{4N_c} N(x, \mathbf{r}_{14}, \mathbf{b}_{14}) - \frac{1}{2N_c} N(x, \mathbf{r}_{34}, \mathbf{b}_{34}) - \frac{3 + 5N_c^2}{4N_c} N(x, \mathbf{r}_{12}, \mathbf{b}_{12}) + \right. \\
&+ \frac{1}{4N_c} \left[N(x, \mathbf{r}_{23}, \mathbf{b}_{23}) - N\left(x, \frac{\alpha_1 \mathbf{r}_{14} + \alpha_3 \mathbf{r}_{34}}{1 - \alpha_2}, \mathbf{b}_{1344}\right) \right] \\
&+ \frac{N_c^2 + 2}{4N_c} N(x, \mathbf{r}_{13}, \mathbf{b}_{13}) + \frac{3N_c^2 - 2}{4N_c} N\left(x, \frac{\alpha_1 \mathbf{r}_{21} + \alpha_3 \mathbf{r}_{23} + \alpha_4 \mathbf{r}_{24}}{1 - \alpha_2}, \mathbf{b}_{1234}\right) \\
&+ \frac{3N_c}{2} N\left(x, \frac{\alpha_3 \mathbf{r}_{13} + \alpha_4 \mathbf{r}_{14}}{\alpha_3 + \alpha_4}, \mathbf{b}_{134}\right) + 2N_c N\left(x, \frac{\alpha_3 \mathbf{r}_{23} + \alpha_4 \mathbf{r}_{24}}{\alpha_3 + \alpha_4}, \mathbf{b}_{234}\right) \\
&+ \frac{N_c^2 + 1}{4N_c} \left[N\left(x, \frac{\alpha_3 \mathbf{r}_{13} + \alpha_4 \mathbf{r}_{14}}{1 - \alpha_2}, \mathbf{b}_{1134}\right) + N(x, \mathbf{r}_{24}, \mathbf{b}_{24}) \right] \\
&- \frac{N_c}{2} \left[N\left(x, \frac{\alpha_4 \mathbf{r}_{34}}{\alpha_3 + \alpha_4}, \mathbf{b}_{334}\right) + N\left(x, -\frac{\alpha_3 \mathbf{r}_{34}}{\alpha_3 + \alpha_4}, \mathbf{b}_{344}\right) \right] \\
&- \frac{N_c}{2} N\left(x, -\frac{\alpha_1 (\alpha_3 \mathbf{r}_{13} + \alpha_4 \mathbf{r}_{14})}{(\alpha_3 + \alpha_4)(\alpha_1 + \alpha_3 + \alpha_4)}, \mathbf{b}_{34,134}\right) \\
&\left. - \frac{N_c^2 - 1}{4N_c} N\left(x, \frac{\alpha_1 \mathbf{r}_{31} + \alpha_4 \mathbf{r}_{34}}{1 - \alpha_2}, \mathbf{b}_{1334}\right) \right\},
\end{aligned} \tag{15}$$

$$\begin{aligned}
\mathcal{N}^{(B)}(\alpha_1, \mathbf{x}_1; \alpha_2, \mathbf{x}_2; \alpha_3, \mathbf{x}_3; \alpha_4, \mathbf{x}_4) &= \\
&= \frac{1}{4} [N(x, \mathbf{r}_{23}, \mathbf{b}_{23}) - N(x, \mathbf{r}_{24}, \mathbf{b}_{24}) + N(x, \mathbf{r}_{3,234}, \mathbf{b}_{2334}) - N(x, \mathbf{r}_{4,234}, \mathbf{b}_{2344}) + \\
&+ 2N(x, \mathbf{r}_{14}, \mathbf{b}_{24}) - 2N(x, \mathbf{r}_{13}, \mathbf{b}_{13})]
\end{aligned} \tag{16}$$

The variables \mathcal{Y}_{ij} in (13, 14) stand for the lab-frame rapidity of quark-antiquark pair made of partons i, j . Explicitly it is given by

$$\mathcal{Y}_{ij} = \ln \left(\frac{(\alpha_i + \alpha_j) q^+}{M_\perp} \right), \tag{17}$$

where α_i and α_j are light-cone fractions of the heavy quarks which form a given quarkonium.

III. NUMERICAL RESULTS

The framework presented in the previous section allows to make unambiguous predictions for the cross-sections. We would like to start the presentation of numerical results with a brief discussion of different uncertainties which

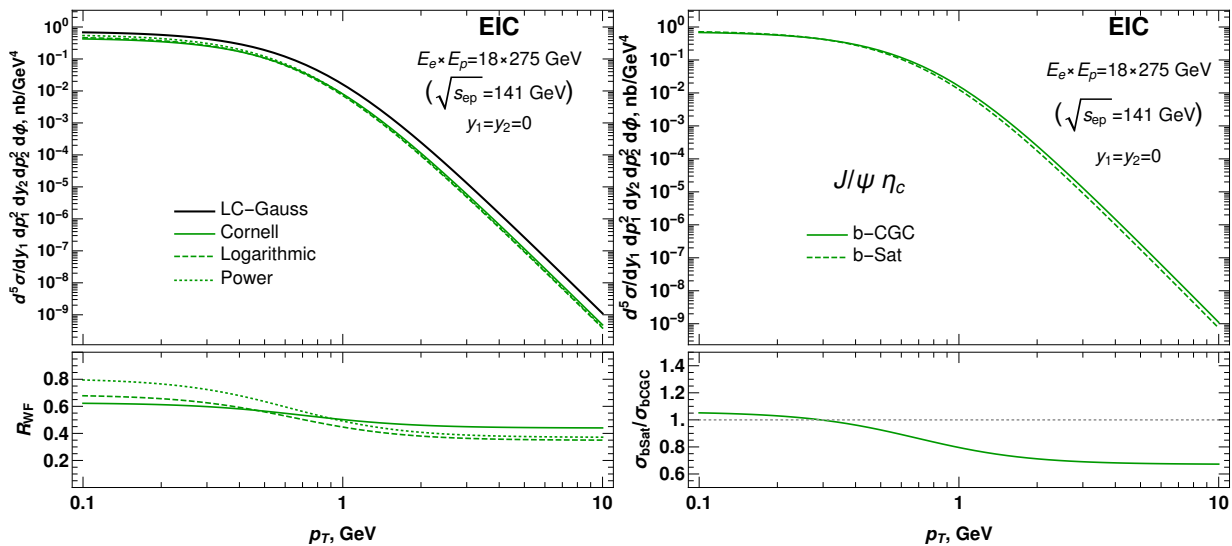


Figure 2. Left plot: Sensitivity of the $J/\psi \eta_c$ production cross-section to the choice of the wave function. We compare results with the LC-Gauss parametrization of the wave function [67, 68] and the wave functions evaluated in potential models [69–72]. In the lower panel of the left figure we show the ratio of the cross-sections from the upper panel to the “LC-Gauss” curve. Right plot: Sensitivity of the $J/\psi \eta_c$ production cross-section to the choice of to the parametrization of the dipole cross-section. In the lower panel of the figure we show the ratio of the cross-sections in b -CGC and b -Sat models. In both plots, for the sake of definiteness, we considered the case when both quarkonia are produced at central rapidities ($y_1 = y_2 = 0$) in the lab frame; for other rapidities and quarkonia pairs the p_T -dependence has similar shape.

are present in our evaluations. For the sake of definiteness, we’ll consider the all-charm sector and focus on $J/\psi + \eta_c$ production, for which the production cross-section is the largest (and thus is easier to study experimentally).

The largest source of uncertainty in our estimates is due to the wave function of the quarkonia, which might be reformulated as uncertainty of the Long Distance Matrix Elements (LDMEs). A popular choice used in phenomenological estimates is the so-called light-cone Gaussian (LC-Gauss) parametrization [67, 68]. This parametrization depends on unknown parameters, which must be fixed from phenomenology. While for J/ψ and Υ mesons these parameters are known or might be fixed from existing experimental data, for heavier mesons, especially for B_c quarkonia, this procedure cannot be applied due to lack of experimental data, thus making it almost impossible to make predictions for heavier mesons. A more systematic approach is to use the wave functions of the quarkonia evaluated in potential models, and using the well-known Brodsky-Huang-Lepage-Terentyev (BHLT) prescription [73–75] to convert the rest frame wave function ψ_{RF} into a light-cone wave function Ψ_{LC} . In the small- r region, which is relevant for estimates, the wave functions of the S -wave heavy quarkonia in different schemes are quite close to each other [76–79], so the uncertainty due to the choice of the potential model should be minimal for physical observables. In order to illustrate this for heavy quarkonia production, in the left panel of Figure 2 we compare predictions for the cross-sections obtained with the LC-Gauss parametrization and various potential models [69–72]. The uncertainty due to the wave function does not exceed 30 per cent, on par with expectations based on $\alpha_s(m_c)$ -counting.

Another source of uncertainty in our evaluations is the choice of parametrization of the dipole amplitude. In the right panel of the Figure 2 we compare predictions obtained with impact parameter (b) dependent “bCGC” [64, 80] and “bSat” [65] parametrizations of the dipole cross-section. In the region of small p_T both parametrizations give very close results. In the region of very large p_T , the difference between the two models increases due to different small- r behavior implemented in “ b -CGC” and “ b -Sat” parametrizations: in the former parametrization the dipole amplitude behaves like $\sim r^\gamma$, whereas in the latter the dependence is much more complicated due to built-in DGLAP evolution of gluon densities in dipole cross-section. In what follows we will use the impact parameter (b) dependent “ b -CGC” parametrization of the dipole cross-section [64, 80],

In Figure 3 we illustrate the p_T -dependence of the cross-section for different quarkonia states (for the sake of definiteness we considered that both quarkonia are produced with the same absolute value of transverse momenta p_T). The strong mass dependence can be understood in the dipole picture: all gluon interactions with dipoles of small size $\sim 1/m_Q$ are strongly suppressed in the heavy quark mass limit, leading to a strong suppression of the cross-sections. As explained in the previous section, the production of $B_c^{*+} B_c^-$ and charmonium-bottomonium pairs

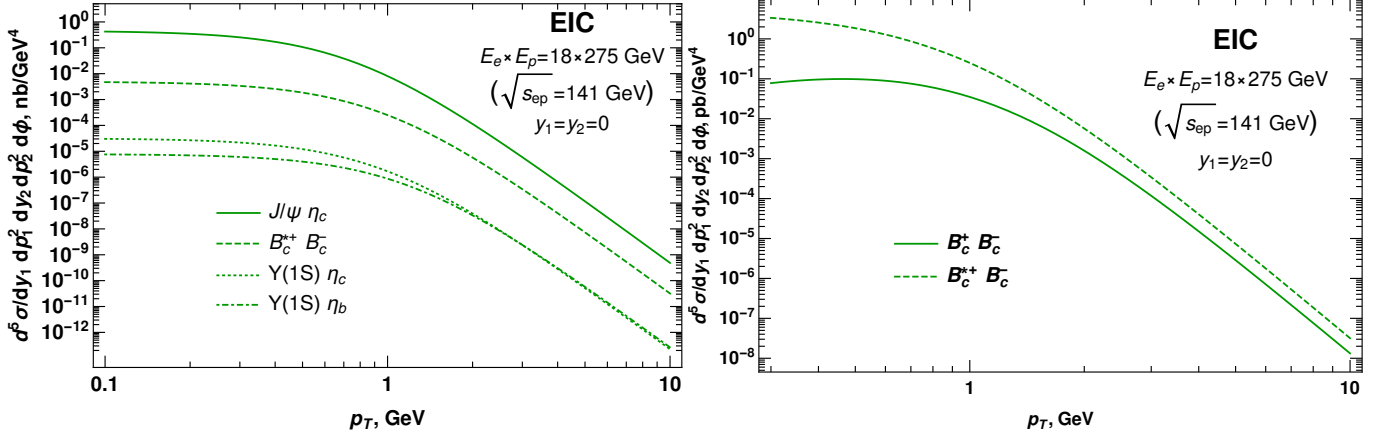


Figure 3. Left plot: Production cross-sections of different quarkonia pairs with spin-parity $(1^-, 0^-)$. The cross-sections differ significantly, due to the heavy constituents masses and wave functions, as well as the classes of diagrams which might contribute. Right plot: Comparison of the cross-sections for $B_c B_c$ meson pairs with different spin-parity: $(1^-, 0^-)$ vs. $(0^-, 0^-)$. For the sake of definiteness we considered the case when both quarkonia are produced at central rapidities ($y_1 = y_2 = 0$) in the lab frame; for other rapidities the p_T -dependence has a similar shape.

get contributions from different classes of diagrams, which explains the significant differences in the cross-sections. The production of bottomonium-bottomonium pairs has significantly smaller cross-sections and does not present any practical interest. For the $B_c^+ B_c^-$ meson pairs, the C -parity does not impose constraints on internal quantum numbers, and for this reason the suggested mechanism might lead to production of both scalar and vector mesons. In the right panel of Figure 4 we can see that the scalar and vector B_c quarkonia should have similar cross-sections at very large p_T , although might differ substantially in the region of small momenta p_T . Potentially this channel might present special interest for searches of the (so far undiscovered) vector mesons $B_c^{*\pm}$.

In Figure 4 we study the dependence of the cross-sections on the azimuthal angle ϕ between the transverse momenta of J/ψ and η_c mesons. For the sake of definiteness, we assumed that transverse momenta $\mathbf{p}_{J/\psi}^\perp, \mathbf{p}_\eta^\perp$ of both quarkonia have equal absolute values. In order to make meaningful comparison of the cross-sections, which differ by orders of magnitude, in the upper row of Figure 4 we plotted the normalized ratio

$$R(\phi) = \frac{d\sigma(\dots, \phi) / dy_1 dp_1^2 dy_2 dp_2^2 d\phi}{d\sigma(\dots, \phi = \pi) / ddy_1 dp_1^2 dy_2 dp_2^2 d\phi}, \quad R(\phi = \pi) \equiv 1 \quad (18)$$

We can see that the ratio has a sharp peak in the back-to-back kinematics ($\phi = \pi$), which minimizes the momentum transfer to the target $|t| = |\Delta^2|$. In contrast, for the angle $\phi \approx 0$, which maximizes the variable $|t| = |\Delta^2|$, the ratio has a pronounced dip. The increase of the peak-to-trough ratio with p_T is due to the higher values of $|t|$ achievable in $\phi \approx 0$ kinematics. For $p_1 \neq p_2$ the dependence on ϕ is qualitatively similar, although the maximum and minimum are less pronounced. The dependence on ϕ has very similar shape for all quarkonia states. Due to smallness of the cross-sections at large p_T , it could be challenging to measure the ratio (18). For this reason, we also analyzed the ratio of the p_T -integrated cross-sections

$$\mathcal{R}(\phi) = \frac{d\sigma(\dots, \phi) / dy_1 dy_2 d\phi}{d\sigma(\dots, \phi = \pi) / ddy_1 dy_2 d\phi}, \quad \mathcal{R}(\phi = \pi) \equiv 1 \quad (19)$$

which should be easier to study experimentally. Its ϕ -dependence is qualitatively similar to that of (18), although is milder. This happens because the p_T -integrated cross-sections get a dominant contribution from the region of relatively small p_T , for which the momentum transfer t remains small for all angles ϕ . We expect that experimental study of the ratios (18,19) could help to understand possible correlations between orientations of the dipole separation vector \mathbf{r} and dipole impact parameter \mathbf{b} in a color singlet dipole amplitude $N(x, \mathbf{r}, \mathbf{b})$. Such dependence is frequently neglected in phenomenological parametrizations, like b -CGC and b -Sat, and for many channels (*e.g.* DIS, DVCS, DVMP) this simplification is justified, since the corresponding cross-sections are not sensitive to the ϕ -dependence. However, in different theoretical models it has been demonstrated that such dependence might exist, and its extraction from data becomes possible if the final state includes *two* hadrons in addition to recoil proton (see [81, 82] for more details). While all previous studies of this dependence focused on exclusive dijet production, the exclusive production

of heavy quarkonia pairs might be also used for this purpose and presents a lot of interest in view of its very clean final state. In order to illustrate feasibility of such measurement, we analyze the modification of the ϕ -dependence of the ratios (18,19) due to possible angular dependence of the dipole amplitude. Following [81], temporarily we'll assume that such dependence is given by the dipole amplitude

$$N(x, \mathbf{r}, \mathbf{b}) \approx N_{b\text{-CGC}}(x, r, b) (1 + 2v_2 \cos(2\theta_{\mathbf{r}, \mathbf{b}})) \quad (20)$$

where $\theta_{\mathbf{r}, \mathbf{b}}$ is the angle between vectors \mathbf{r} and \mathbf{b} , and v_2 is a numerical constant which characterizes the size of angular dependent term. In the left panel of the Figure 5 we illustrate the ϕ -dependence of the ratio $\mathcal{R}(\phi)$ for different values of v_2 . Since expected values of v_2 are very small (of order a few percent), the shape of $\mathcal{R}(\phi)$ experiences only small changes. For this reason, extraction of the constant v_2 from quarkonia pair production requires to use special observables which would enhance sensitivity to v_2 . We suggest to use for this purpose the geometric mean

$$\mathcal{G}(\phi) = \sqrt{\mathcal{R}(\phi)\mathcal{R}(\pi - \phi)}. \quad (21)$$

The strong ϕ -dependence of the cross-sections, which is due to increase of momentum transfer t to the recoil proton, largely cancels in $\mathcal{G}(\phi)$, and thus extraction of v_2 from this observable might be done with better precision. Indeed, for small t , the dependence of the cross-sections on t might be approximated with exponent,

$$R(\phi) \sim e^{Bt} \sim e^{-B(\mathbf{p}_1^+ + \mathbf{p}_2^+)^2} \sim e^{-B[(p_1^+)^2 + (p_2^+)^2]} e^{-2Bp_1^+ p_2^+ \cos \phi}. \quad (22)$$

In the product $R(\phi)R(\pi - \phi)$ the exponents with ϕ -dependence cancel, thus giving possibility to study the ‘‘residual’’ ϕ -dependence due to $\mathcal{O}(v_2)$ -terms in prefactors. The extension of this proof for the p_T -integrated ratios, which appear in (21), is straightforward. As we can see from the right panel of the Figure 5, the observable $\mathcal{G}(\phi)$ indeed has significantly milder dependence on ϕ , and thus is much better suited for extraction of v_2 .

Finally, in the Figure 6 we show the dependence of the cross-section on the quarkonia rapidities, integrated over the transverse momenta of both heavy mesons. In the left panel we consider the special case when both quarkonia are produced with the same rapidities $y_1 = y_2$ in the lab frame. The dependence on y_i in this setup merely reflects the dependence on the invariant photon-proton energy, as could be seen from (10). In the right panel of the same Figure 6 we show the dependence of the cross-section on the rapidity difference Δy between the two heavy mesons. For the sake of definiteness we consider that both quarkonia have opposite rapidities in the lab frame, $y_1 = -y_2 = \Delta y/2$. In this setup the variable Δy might be unambiguously related to the invariant mass of the heavy quarkonia pair using (11). We may observe that in this case the cross-section becomes suppressed as a function of Δy , which illustrates the fact that the quarkonia are predominantly produced with the same rapidities. Finally, in Figure 7 we show predictions for the pair production in the kinematics of ultraperipheral collisions at LHC. For the sake of definiteness, we consider proton-lead collisions. Qualitatively the behavior of the cross-section is similar to that of ep production.

IV. CONCLUSIONS

In this manuscript we have studied in detail the exclusive photoproduction of heavy quarkonia pairs, which include bottom mesons. We focused on the leading order contribution, which leads to production of charmonia and bottomonia pairs with opposite C -parities. For $B_c^+ B_c^-$ pairs, the C -parity does not impose any constraints on the internal quantum numbers of quarkonia, so the suggested mechanism might be used as a clean channel for studies of (so far undiscovered) B_c mesons with different internal quantum numbers. The analysis of mixed charm-bottom pairs (e.g. $B_c^+ B_c^-$ or $J/\psi \eta_b$, $\Upsilon \eta_c$ pairs) allows to single out contributions of two main classes of diagrams in the suggested production mechanism. In all cases the quarkonia are produced with relatively small opposite transverse momenta p_T , and small separation in rapidity: the kinematic which minimizes the momentum transfer to the recoil proton and the invariant mass of the produced pair. The dependence of the cross-section on azimuthal angle between transverse momenta of produced quarkonia might present special interest, since it allows to test the dependence of the dipole amplitude $N(x, \mathbf{r}, \mathbf{b})$ on the relative angle between the dipole separation \mathbf{r} and impact parameter \mathbf{b} . We estimated numerically the cross-sections in the kinematics of ultraperipheral collisions at LHC and the kinematics of the forthcoming Electron-Ion Collider. We found that $J/\psi \eta_c$ and $B_c^+ B_c^-$ might be studied with reasonable precision in forthcoming experiments. The production cross-sections of other quarkonia pairs, especially from the all-bottom states (like e.g. $\Upsilon \eta_b$) are numerically significantly smaller due to extra suppression by the heavy mass and a different production mechanism.

ACKNOWLEDGEMENTS

We thank our colleagues at UTFSM university for encouraging discussions. This research was partially supported by Proyecto ANID PIA/APOYO AFB180002 (Chile) and Fondecyt (Chile) grant 1220242. The research of S. Andrade

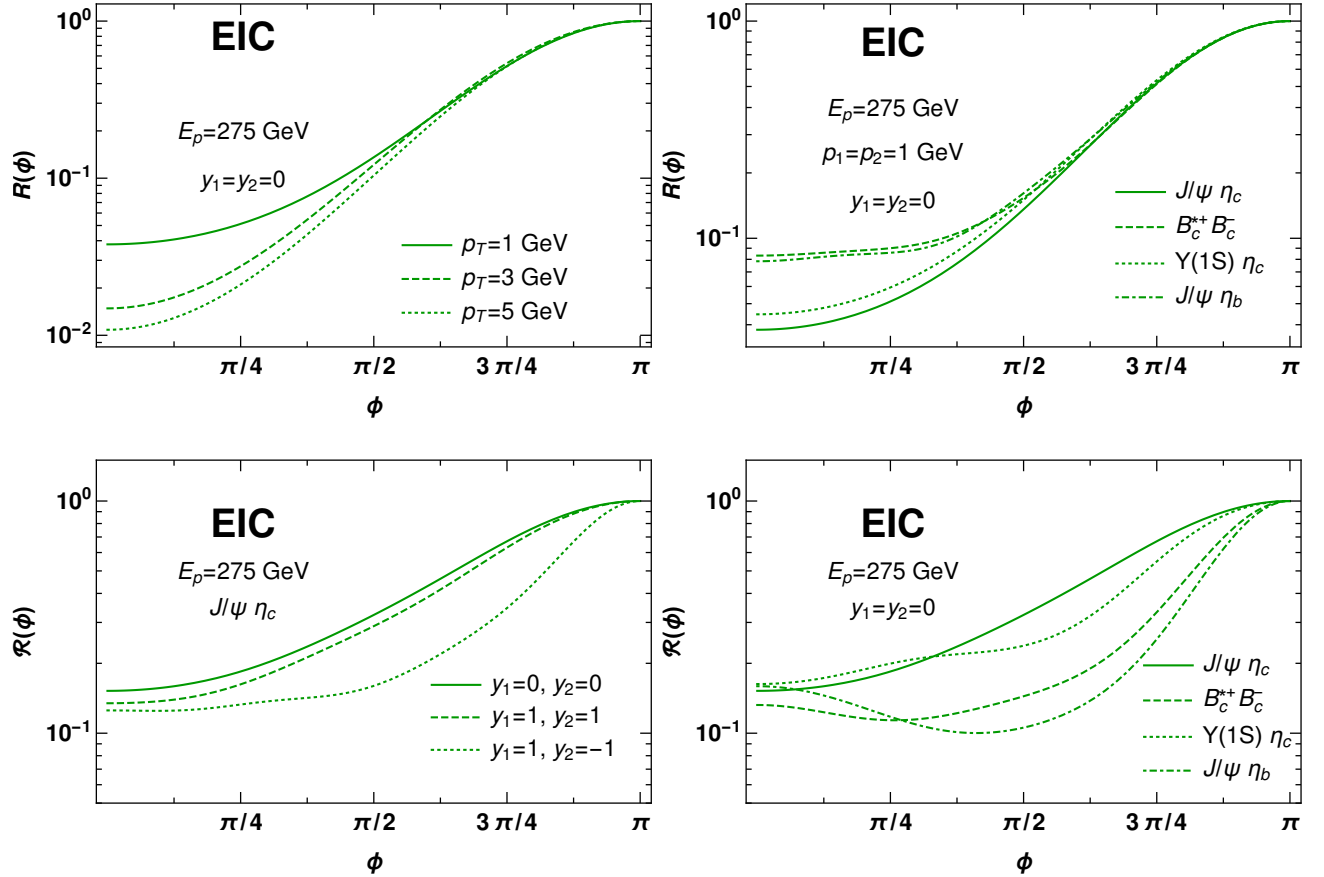


Figure 4. Upper row: Dependence of the normalized ratio $R(\phi)$, defined in (18), on the angle ϕ (difference between azimuthal angles of both quarkonia). The left plot corresponds to $J/\psi \eta_c$ pair production, but with different transverse momenta. The right plot corresponds to different quarkonia states, and fixed absolute values of the transverse momentum p_T . Lower row: Similar dependence of p_T -integrated ratio $\mathcal{R}(\phi)$, defined in (19), on the angle ϕ . In the left plot we compare the predictions for $J/\psi \eta_c$ with different rapidities; in the right plot we compare the predictions for different quarkonia pairs, at fixed central rapidity in the lab frame. The appearance of the sharp peak in back-to-back kinematics is explained in the text. For other rapidities the p_T -dependence has similar shape.

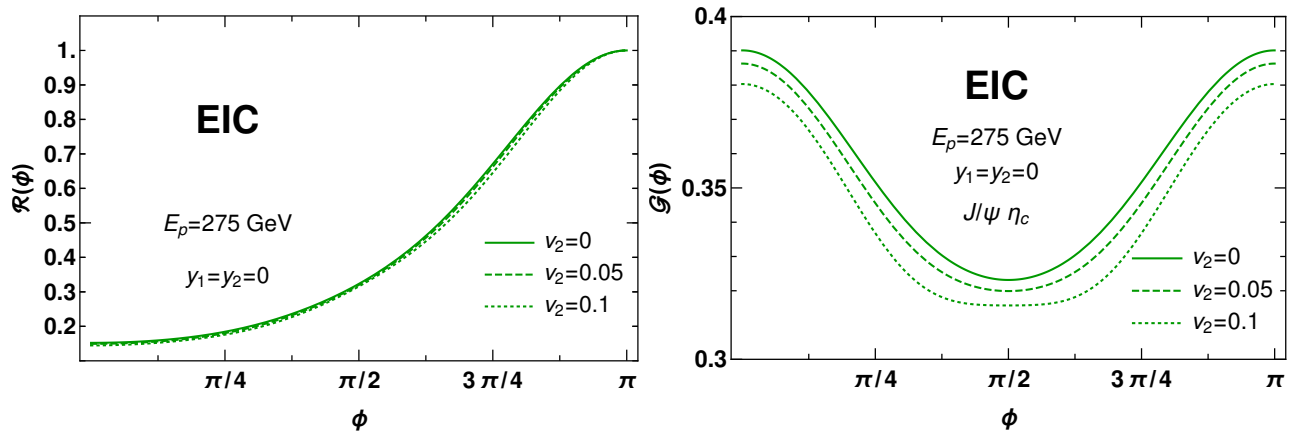


Figure 5. Left plot: The dependence of the p_T -integrated ratio $\mathcal{R}(\phi)$ defined in (19) on the angle ϕ (azimuthal angle between quarkonia). The curves differ by choice of the parameter v_2 defined in (20). Right plot: Similar dependence for the geometric mean $\mathcal{G}(\phi)$ defined in (21). Both plots correspond to $J/\psi \eta_c$ pair production at central rapidities ($y_1 = y_2 = 0$). For other quarkonia pairs the ϕ -dependence has similar shape.

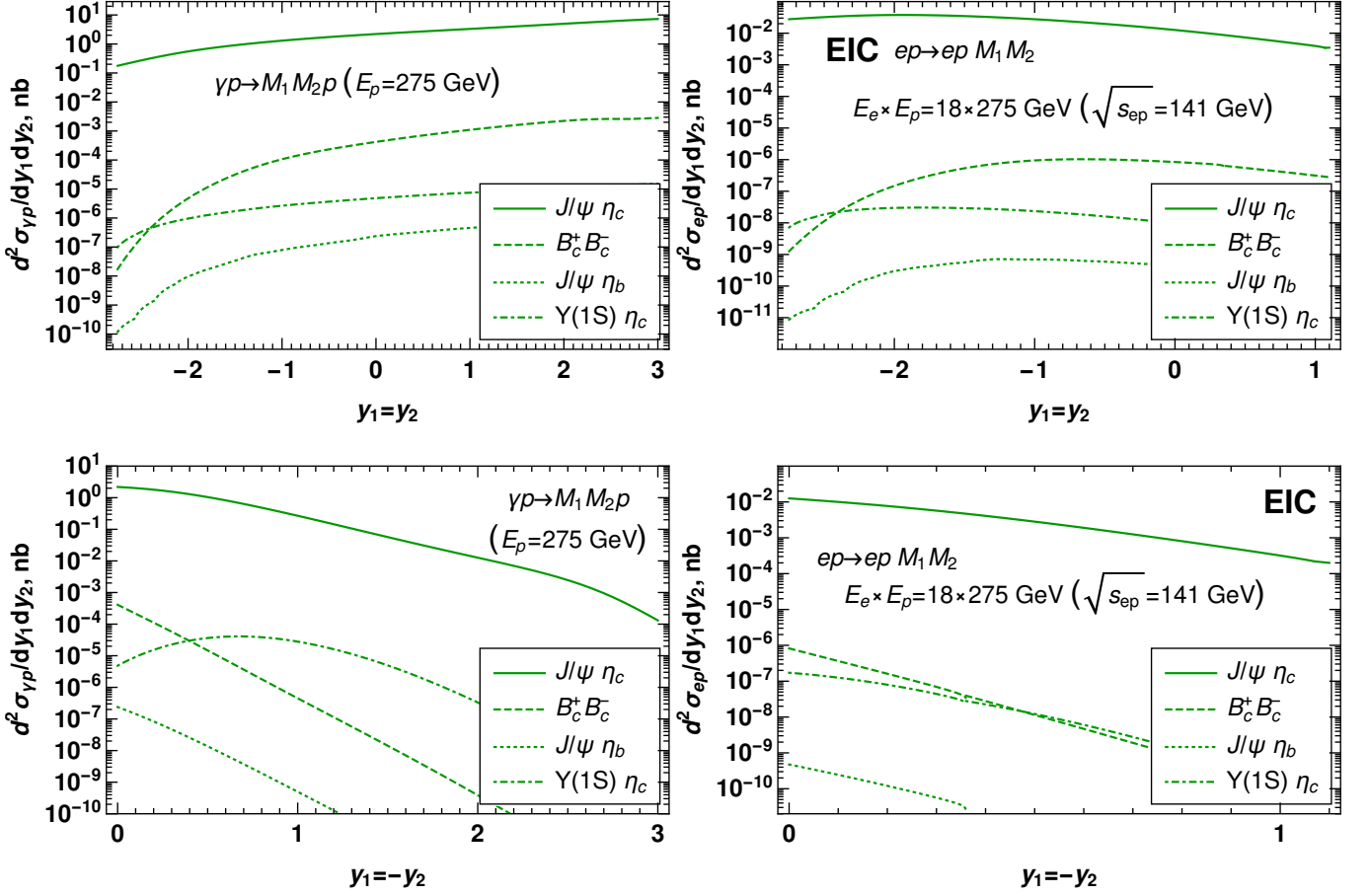


Figure 6. The rapidity dependence of the photoproduction cross-section in EIC kinematics. The plots in the upper row correspond to a configuration with equal rapidities of the produced quarkonia, $y_1 = y_2$, whereas the lower row corresponds to rapidities which differ by a sign in the lab frame, $y_1 = -y_2$. In both rows the left column corresponds to cross-section of photoproduction subprocess, $\gamma p \rightarrow M_1 M_2 p$, whereas the right column corresponds to a cross-section of the electroproduction process $ep \rightarrow M_1 M_2 ep$ and takes into account an additional leptonic factor, as defined in (1).

was also partially supported by the Fellowship Program ANID BECAS/MAGÍSTER NACIONAL (Chile) 22200123. "Powered@NLHPC: This research was partially supported by the supercomputing infrastructure of the NLHPC (ECM-02)".

Appendix A: Evaluation of the photon wave function

The evaluation of the photon wave function follows the standard light-cone rules formulated in [16, 83]. The result for the $\bar{Q}Q$ component is well-known in the literature [67, 84]. The wave function of the $\bar{Q}Q\bar{Q}Q$ -component might be expressed in terms of the wave function of $\bar{Q}Q$ -component. The dominant contribution [?] to the electroproduction and photoproduction in ultraperipheral kinematics comes from quasireal transversely polarized photons, for this reason in what follows we'll focus on the contribution of on-shell photons. The expression for the momentum of the photon (4) simplifies in this case and has only light-cone components in the direction of plus-axis,

$$q \approx (q^+, 0, \mathbf{0}_\perp). \quad (\text{A1})$$

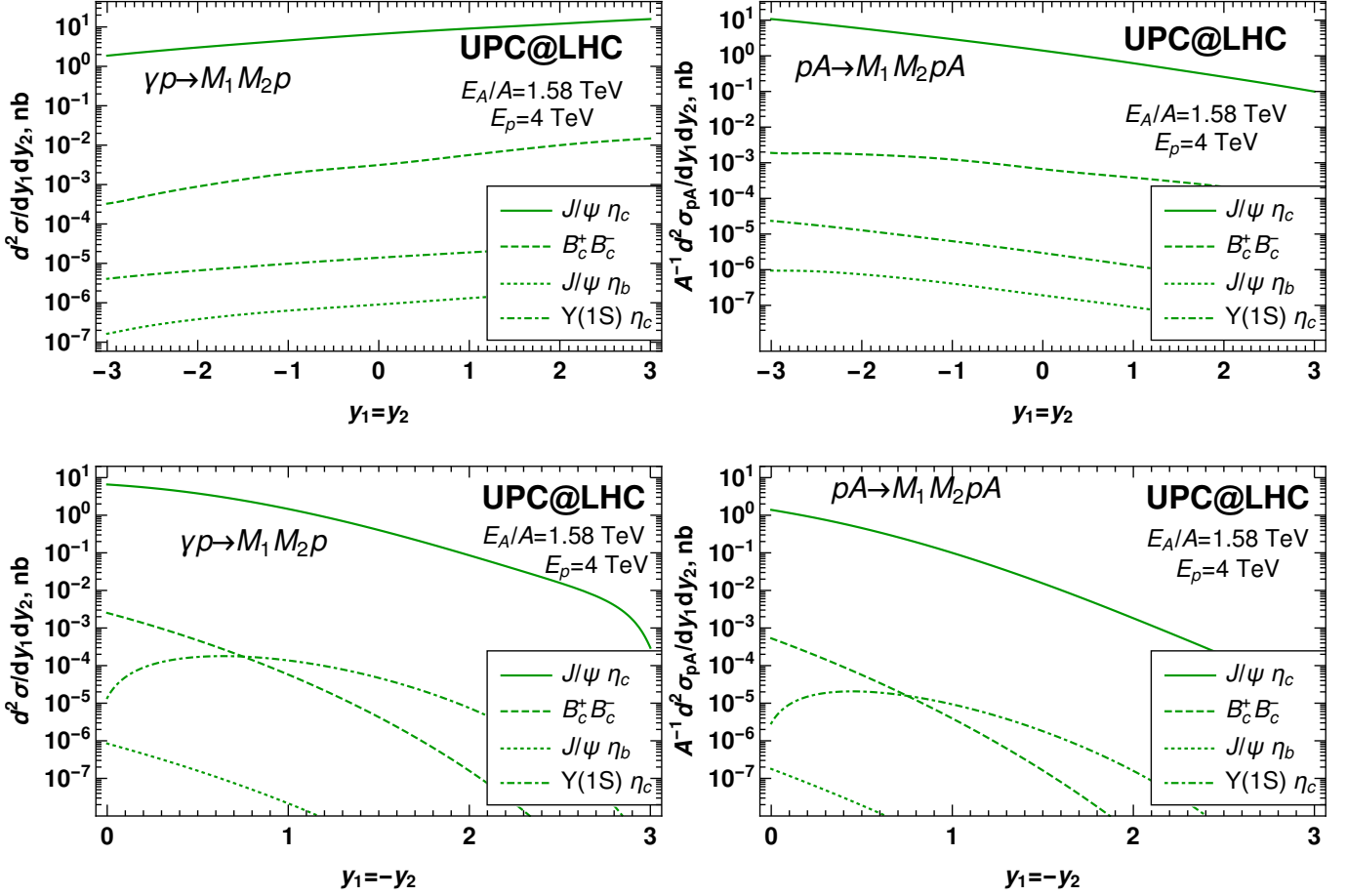


Figure 7. The rapidity dependence of the photoproduction cross-section in the kinematics of the ultraperipheral collisions at LHC. The plots in the upper row correspond to a configuration with equal rapidities of the produced quarkonia, $y_1 = y_2$, whereas the lower row corresponds to rapidities which differ by a sign in lab frame, $y_1 = -y_2$. In both rows the left plot corresponds to the *photoproduction* cross-section, and the right column shows predictions for the cross-section of the full process $pA \rightarrow pAM_1M_2$, as defined in (2).

The polarization vector of the transversely polarized photon is given by

$$\varepsilon_T^\mu(q) \equiv \left(0, \frac{\mathbf{q}_\perp \cdot \boldsymbol{\varepsilon}_\gamma}{q^+}, \varepsilon_\gamma \right) \approx (0, 0, \varepsilon_\gamma), \quad (\text{A2})$$

$$\varepsilon_\gamma = \frac{1}{\sqrt{2}} \begin{pmatrix} 1 \\ \pm i \end{pmatrix}, \quad \gamma = \pm 1. \quad (\text{A3})$$

where in (A2) we took into account that $\mathbf{q}_\perp = 0$. Before interaction with the target, the photon might fluctuate into a virtual quark-antiquark pairs, as well as into gluons. In configuration space the wave function of the $\bar{Q}Q$ state is given by [67, 84]

$$\Psi_{h\bar{h}}^\lambda(z, \mathbf{r}_{12}, m_q, a) = -\frac{2}{(2\pi)} \left[(z\delta_{\lambda,h} - (1-z)\delta_{\lambda,-h}) \delta_{h,-\bar{h}} i\varepsilon_\lambda \cdot \nabla - \frac{m_q}{\sqrt{2}} \text{sign}(h)\delta_{\lambda,h}\delta_{h,\bar{h}} \right] K_0(a\mathbf{r}_{12}). \quad (\text{A4})$$

where z is the fraction of the photon momentum carried by the quark, and \mathbf{r}_{12} is the transverse distance between quark and antiquark.

The $\bar{Q}Q\bar{Q}Q$ component of the photon wave function has been evaluated in detail in our earlier paper [66], and the final result will be given here for the sake of completeness. In leading order over α_s the wave functions obtain contributions from the two diagrams shown in the Figure (8). For the sake of generality we will assume that the produced quark-antiquark pairs have different flavors, and will use the notations m_1 for the current mass of the quark

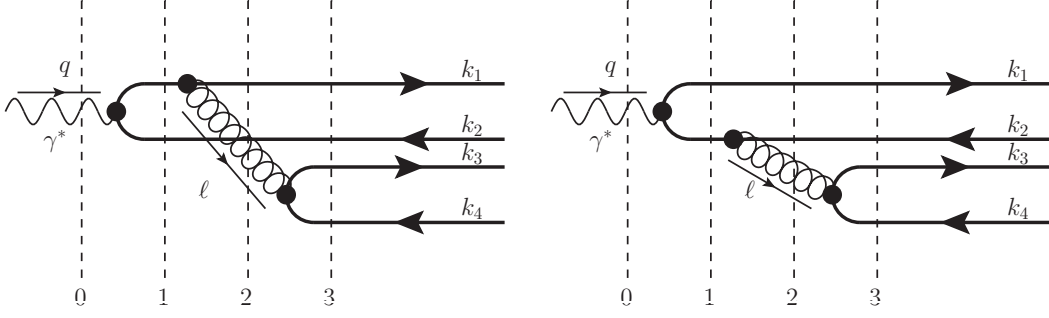


Figure 8. The leading order contribution to the wave function $\psi_{\bar{Q}Q\bar{Q}Q}^{(\gamma)}$ defined in the text. The momenta k_i shown in the right-hand side are Fourier conjugates of the coordinates x_i . It is implied that both diagrams should be supplemented by all possible permutations of final state quarks (see the text for more details).

line connected to a photon, and m_2 for the current masses of the quark-antiquark pair produced from the virtual gluon. The evaluation of the diagrams follows the standard rules of the light-cone perturbation theory [16, 83]. The wave function might be represented as a sum

$$\psi_{\bar{Q}Q\bar{Q}Q}^{(\gamma)} = \psi_{\bar{Q}Q\bar{Q}Q}^{(\gamma, \text{noninst})} + \psi_{\bar{Q}Q\bar{Q}Q}^{(\gamma, \text{inst})} \quad (\text{A5})$$

where the first and the second terms correspond to contributions of non-instantaneous and instantaneous parts of propagators of all virtual particles, and for the sake of brevity we omitted color and helicity indices of heavy quarks (c_i and a_i respectively). The non-instantaneous contribution is given by the sum

$$\psi_{\bar{Q}Q\bar{Q}Q}^{(\gamma, \text{noninst})}(\{\alpha_i, \mathbf{x}_i\}) = A(\{\alpha_i, \mathbf{x}_i\}) + B(\{\alpha_i, \mathbf{x}_i\}). \quad (\text{A6})$$

where

$$\begin{aligned} A(\{\alpha_i, \mathbf{r}_i\}) = & -\frac{2e_q\alpha_s(\mu)(t_a)_{c_1c_2} \otimes (t_a)_{c_3c_4}}{\pi^3(1-\alpha_1-\alpha_2)^2\sqrt{\alpha_1\alpha_2}} \int \frac{q_1 dq_1 k_2 dk_2}{\frac{\bar{\alpha}_2 q_1^2}{\alpha_1(1-\alpha_1-\alpha_2)} + \frac{m_1^2(\alpha_1+\alpha_2)}{\alpha_1\alpha_2} + \frac{k_2^2}{\alpha_2\bar{\alpha}_2}} \times \\ & \times \frac{1}{k_2^2 + m_1^2} \sqrt{\frac{\alpha_2}{\alpha_1}} [(\alpha_2\delta_{\gamma, a_2} - \bar{\alpha}_2\delta_{\gamma, -a_2})(\bar{\alpha}_2\delta_{\lambda, a_1} + \alpha_1\delta_{\lambda, -a_1})\delta_{a_1, -a_2} \times \\ & \times (\mathbf{n}_{2,134} \cdot \boldsymbol{\varepsilon}_\gamma)(\mathbf{n}_{1,34} \cdot \boldsymbol{\varepsilon}_\lambda^*) k_2 J_1(k_2|\mathbf{x}_2 - \mathbf{b}_{134}|) q_1 J_1(q_1|\mathbf{x}_1 - \mathbf{b}_{34}|) + \\ & + \frac{m_q^2}{2} \delta_{\lambda, -a_1} \delta_{\gamma, a_2} \delta_{a_1, -a_2} J_0(k_2|\mathbf{x}_2 - \mathbf{b}_{134}|) J_0(q_1|\mathbf{x}_1 - \mathbf{b}_{34}|) \frac{(1-\alpha_1-\alpha_2)^2}{1-\alpha_2} \\ & - \frac{im_q}{\sqrt{2}} \text{sign}(a_2) \delta_{\gamma, a_2} \delta_{a_1, a_2} (\bar{\alpha}_2\delta_{\lambda, a_1} + \alpha_1\delta_{\lambda, -a_1}) \times \\ & \times \mathbf{n}_{1,34} \cdot \boldsymbol{\varepsilon}_\lambda^* q_1 J_1(q_1|\mathbf{x}_1 - \mathbf{b}_{34}|) J_0(k_2|\mathbf{x}_2 - \mathbf{b}_{134}|) \\ & - \frac{im_q}{\sqrt{2}} \text{sign}(a_1) \delta_{\lambda, -a_1} (\alpha_2\delta_{\gamma, a_2} - \bar{\alpha}_2\delta_{\gamma, -a_2}) \delta_{a_1, a_2} \frac{(1-\alpha_1-\alpha_2)^2}{1-\alpha_2} \times \\ & \times (\mathbf{n}_{2,134} \cdot \boldsymbol{\varepsilon}_\gamma) k_2 J_1(k_2|\mathbf{x}_2 - \mathbf{b}_{134}|) J_0(q_1|\mathbf{x}_1 - \mathbf{b}_{34}|) \times \\ & \times \Psi_{a_3, a_4}^{-\lambda} \left(\frac{\alpha_3}{\alpha_3 + \alpha_4}, \mathbf{r}_{34}, m_2, \sqrt{m_2^2 + \frac{\alpha_3\alpha_4}{\alpha_3 + \alpha_4} \left[\frac{\bar{\alpha}_2 q_1^2}{\alpha_1(1-\alpha_1-\alpha_2)} + \frac{m_1^2(\alpha_1+\alpha_2)}{\alpha_1\alpha_2} + \frac{k_2^2}{\alpha_2\bar{\alpha}_2} \right]} \right) \end{aligned} \quad (\text{A7})$$

and

$$B(\alpha_1, \mathbf{x}_1, \alpha_2, \mathbf{x}_2, \alpha_3, \mathbf{x}_3, \alpha_4, \mathbf{x}_4) = -A(\alpha_2, \mathbf{x}_2, \alpha_1, \mathbf{x}_1, \alpha_4, \mathbf{x}_4, \alpha_3, \mathbf{x}_3).$$

The variable $\mathbf{b}_{j_1 \dots j_n}$ corresponds to the center of mass position of the n partons j_1, \dots, j_n . The variable $\mathbf{n}_{i, j_1 \dots j_n} = (\mathbf{x}_i - \mathbf{b}_{j_1 \dots j_n}) / |\mathbf{x}_i - \mathbf{b}_{j_1 \dots j_n}|$ is a unit vector pointing from quark i towards the center-of-mass of the system of quarks $j_1 \dots j_n$. The tree-like structure of the leading order diagrams 1, 2 in Fig. 8 and iterative evaluation of the coordinate of the center of mass of two partons $\mathbf{b}_{ij} = (\alpha_i \mathbf{r}_i + \alpha_j \mathbf{r}_j) / (\alpha_i + \alpha_j)$, allows to reconstruct the transverse coordinates

of all intermediate partons. The variables $\mathbf{r}_1 - \mathbf{b}_{34}$ and $\mathbf{r}_2 - \mathbf{b}_{34}$ physically have the meaning of the relative distance between the recoil quark or antiquark and the emitted gluon. Similarly, the variables $\mathbf{r}_1 - \mathbf{b}_{234}$ and $\mathbf{r}_2 - \mathbf{b}_{134}$ might be interpreted as the size of $\bar{Q}Q$ pair produced right after splitting of the incident photon.

Similarly, for the instantaneous contributions it is possible to get

$$\begin{aligned} \psi_{\bar{Q}Q\bar{Q}Q}^{(\gamma,\text{inst.})}(\{\alpha_i, \mathbf{r}_i\}) &= A_g(\{\alpha_i, \mathbf{r}_i\}) + B_g(\{\alpha_i, \mathbf{r}_i\}) + \\ &+ A_q(\{\alpha_i, \mathbf{r}_i\}) + B_q(\{\alpha_i, \mathbf{r}_i\}), \end{aligned} \quad (\text{A8})$$

where the subscript indices q, g in the right-hand side denote the parton propagator which should be taken instantaneous (q for quark, g for gluon), and

$$\begin{aligned} A_g(\{\alpha_i, \mathbf{r}_i\}) &= -\frac{e_q \alpha_s(m_Q) (t_a)_{c_1 c_2} \otimes (t_a)_{c_3 c_4}}{\pi^4 (1 - \alpha_1 - \alpha_2)^3} \int q_1 dq_1 k_2 dk_2 J_0(q_1 |\mathbf{r}_1 - \mathbf{b}_{34}|) \times \\ &\times \frac{1}{\mathbf{k}_{2\perp}^2 + m_1^2} [(\alpha_2 \delta_{\gamma, a_1} - \bar{\alpha}_2 \delta_{a_1, -\gamma}) \delta_{a_1, -a_2} i \mathbf{n}_{2,134} \cdot \boldsymbol{\varepsilon}_\gamma k_2 J_1(k_2 |\mathbf{r}_2 - \mathbf{b}_{134}|) \\ &+ \frac{m_q}{\sqrt{2}} \text{sign}(a_1) \delta_{\gamma, a_1} \delta_{a_1, a_2} J_0(k_2 |\mathbf{r}_2 - \mathbf{b}_{134}|)] \alpha_3 \alpha_4 \delta_{a_3, -a_4} K_0(a_{34} r_{34}). \end{aligned} \quad (\text{A9})$$

$$\begin{aligned} A_q(\{\alpha_i, \mathbf{r}_i\}) &= -\frac{e_q \alpha_s(m_q) (t_a)_{c_1 c_2} \otimes (t_a)_{c_3 c_4}}{2\pi^4 (1 - \alpha_1 - \alpha_2)^2 \bar{\alpha}_2} \delta_{a_1, -a_2} \delta_{\gamma, -a_1} \int q_1 dq_1 k_2 dk_2 \frac{J_0(q_1 |\mathbf{r}_1 - \mathbf{b}_{34}|) J_0(k_2 |\mathbf{r}_2 - \mathbf{b}_{134}|)}{D_2(\alpha_1, \mathbf{k}_1; \alpha_2, \mathbf{k}_2)} \times \\ &\times \left[-(\alpha_3 \delta_{-\gamma, a_3} - \alpha_4 \delta_{\gamma, a_3}) \delta_{a_3, -a_4} i \boldsymbol{\varepsilon}_\gamma \cdot \mathbf{n}_{34} a_{34} K_1(a_{34} r_{34}) - \frac{m_q(\alpha_3 + \alpha_4)}{\sqrt{2}} \text{sign}(a_3) \delta_{\gamma, -a_3} \delta_{a_3, a_4} K_0(a_{34} r_{34}) \right] \end{aligned} \quad (\text{A10})$$

$$a_{34}(q_1, k_2) \equiv \sqrt{m_2^2 + \frac{\alpha_3 \alpha_4}{\alpha_3 + \alpha_4} \left[\frac{\bar{\alpha}_2 q_1^2}{\alpha_1 (1 - \alpha_1 - \alpha_2)} + \frac{m_1^2 (\alpha_1 + \alpha_2)}{\alpha_1 \alpha_2} + \frac{k_2^2}{\alpha_2 \bar{\alpha}_2} \right]} \quad (\text{A11})$$

and the functions B_q, B_g might be obtained from A_q, A_g using

$$B_i(\alpha_1, \mathbf{x}_1, \alpha_2, \mathbf{x}_2, \alpha_3, \mathbf{x}_3, \alpha_4, \mathbf{x}_4) = -A_i(\alpha_2, \mathbf{x}_2, \alpha_1, \mathbf{x}_1, \alpha_4, \mathbf{x}_4, \alpha_3, \mathbf{x}_3), \quad i = q, g. \quad (\text{A12})$$

-
- [1] J. G. Korner and G. Thompson, Phys. Lett. B **264**, 185 (1991).
[2] M. Neubert, “Heavy quark symmetry,” Phys. Rept. **245** (1994), 259-396 [arXiv:hep-ph/9306320 [hep-ph]].
[3] G. T. Bodwin, E. Braaten and G. P. Lepage, Phys. Rev. D **51**, 1125 (1995) Erratum: [Phys. Rev. D **55**, 5853 (1997)] [hep-ph/9407339].
[4] F. Maltoni, M. L. Mangano and A. Petrelli, Nucl. Phys. B **519**, 361 (1998) [hep-ph/9708349].
[5] N. Brambilla, E. Mereghetti and A. Vairo, Phys. Rev. D **79**, 074002 (2009) Erratum: [Phys. Rev. D **83**, 079904 (2011)] [arXiv:0810.2259 [hep-ph]].
[6] Y. Feng, J. P. Lansberg and J. X. Wang, Eur. Phys. J. C **75**, no. 7, 313 (2015) [arXiv:1504.00317 [hep-ph]].
[7] N. Brambilla *et al.*; Eur. Phys. J. C **71**, 1534 (2011).
[8] P. L. Cho and A. K. Leibovich, Phys. Rev. D **53**, 6203 (1996) [hep-ph/9511315].
[9] P. L. Cho and A. K. Leibovich, Phys. Rev. D **53**, 150 (1996) [hep-ph/9505329].
[10] S. P. Baranov, Phys. Rev. D **66**, 114003 (2002).
[11] S. P. Baranov and A. Szczurek, Phys. Rev. D **77**, 054016 (2008) [arXiv:0710.1792 [hep-ph]].
[12] S. P. Baranov, A. V. Lipatov and N. P. Zotov, Phys. Rev. D **85**, 014034 (2012) [arXiv:1108.2856 [hep-ph]].
[13] S. P. Baranov and A. V. Lipatov, Phys. Rev. D **96**, no. 3, 034019 (2017) [arXiv:1611.10141 [hep-ph]].
[14] S.P. Baranov, A.V. Lipatov, N.P. Zotov; Eur. Phys. J. C **75**, 455 (2015).
[15] S. J. Brodsky, G. Kopp and P. M. Zerwas, “Hadron Production Near Threshold in Photon-photon Collisions,” Phys. Rev. Lett. **58** (1987), 443.
[16] G. P. Lepage and S. J. Brodsky, “Exclusive processes in perturbative quantum chromodynamics,” Phys. Rev. D **22** (1980) 2157.
[17] C. Berger and W. Wagner, “Photon-Photon Reactions,” Phys. Rept. **146** (1987), 1-134.
[18] M. S. Baek, S. Y. Choi and H. S. Song, “Exclusive heavy meson pair production at large recoil,” Phys. Rev. D **50** (1994), 4363-4371.

- [19] Y. Bai, S. Lu and J. Osborne, arXiv:1612.00012 [hep-ph].
- [20] W. Heupel, G. Eichmann and C. S. Fischer, Phys. Lett. B **718**, 545 (2012) [arXiv:1206.5129 [hep-ph]].
- [21] R. J. Lloyd and J. P. Vary, Phys. Rev. D **70**, 014009 (2004) [hep-ph/0311179].
- [22] J. Vijande, N. Barnea and A. Valcarce, Int. J. Mod. Phys. A **22**, 561 (2007) [hep-ph/0610124].
- [23] J. Vijande, A. Valcarce and J.-M. Richard, Few Body Syst. **54**, 1015 (2013) [arXiv:1212.4273 [hep-ph]].
- [24] X. Chen, “Fully-heavy tetraquarks: $bb\bar{c}\bar{c}$ and $cb\bar{c}\bar{c}$,” Phys. Rev. D **100** (2019) no.9, 094009 [arXiv:1908.08811 [hep-ph]].
- [25] A. Esposito and A. D. Polosa, “A $bb\bar{b}\bar{b}$ di-bottomonium at the LHC,” Eur. Phys. J. C **78** (2018) no.9, 782 [arXiv:1807.06040 [hep-ph]].
- [26] R. Cardinale [LHCb], “LHCb spectroscopy results,” PoS LHCP2018 (2018), 191
- [27] R. Aaij *et al.* [LHCb], “Search for beautiful tetraquarks in the $\Upsilon(1S)\mu^+\mu^-$ invariant-mass spectrum,” JHEP **10** (2018), 086 [arXiv:1806.09707 [hep-ex]].
- [28] L. Capriotti [LHCb], “Spectroscopy of Heavy Hadrons at LHCb,” J. Phys. Conf. Ser. **1137** (2019) no.1, 012004
- [29] R. Aaij *et al.* [LHCb], “Observation of structure in the J/ψ -pair mass spectrum,” Sci. Bull. **65** (2020) no.23, 1983-1993 [arXiv:2006.16957 [hep-ex]].
- [30] A. Accardi *et al.*, Eur. Phys. J. C **52**, no. 9, 268 (2016) [arXiv:1212.1701 [nucl-ex]].
- [31] Press release at the website of the United States Department of Energy: <https://www.energy.gov/articles/us-department-energy-selects-brookhaven-national-laboratory-host-major-new-nuclear-physics>.
- [32] Press-release at the website of the Brookhaven National Laboratory (BNL): <https://www.bnl.gov/newsroom/news.php?a=116998>.
- [33] R. Abdul Khalek *et al.* “Science Requirements and Detector Concepts for the Electron-Ion Collider: EIC Yellow Report,” [arXiv:2103.05419 [physics.ins-det]].
- [34] J.L. Abelleira Fernandez *et al.* [LHeC Study Group]; J. Phys. G **39**, 075001 (2012).
- [35] M. Mangano, CERN Yellow Reports: Monographs, 3/2017; doi:10.23731/CYRM-2017-003 [arXiv:1710.06353 [hep-ph]], ISBN: 9789290834533 (Print), 9789290834540 (eBook).
- [36] P. Agostini *et al.* [LHeC and FCC-he Study Group], “The Large Hadron-Electron Collider at the HL-LHC,” [arXiv:2007.14491 [hep-ex]].
- [37] A. Abada *et al.* [FCC], Eur. Phys. J. C **79** (2019) no.6, 474.
- [38] V. P. Goncalves, B. D. Moreira and F. S. Navarra, “Double vector meson production in $\gamma\gamma$ interactions at hadronic colliders,” Eur. Phys. J. C **76** (2016) no.3, 103 [arXiv:1512.07482 [hep-ph]].
- [39] V. Goncalves and R. Palota da Silva, “Exclusive and diffractive quarkonium - pair production at the LHC and FCC,” Phys. Rev. D **101** (2020) no.3, 034025 [arXiv:1912.02720 [hep-ph]].
- [40] V. P. Goncalves and M. V. T. Machado, “Dipole model for double meson production in two-photon interactions at high energies,” Eur. Phys. J. C **49** (2007), 675-684 [arXiv:hep-ph/0605304 [hep-ph]].
- [41] S. Baranov, A. Cisek, M. Klusek-Gawenda, W. Schafer and A. Szczurek, “The $\gamma\gamma \rightarrow J/\psi J/\psi$ reaction and the $J/\psi J/\psi$ pair production in exclusive ultraperipheral ultrarelativistic heavy ion collisions,” Eur. Phys. J. C **73** (2013) no.2, 2335 [arXiv:1208.5917 [hep-ph]].
- [42] H. Yang, Z. Q. Chen and C. F. Qiao, “NLO QCD corrections to exclusive quarkonium-pair production in photon-photon collision,” Eur. Phys. J. C **80** (2020) no.9, 806.
- [43] V. P. Goncalves, B. D. Moreira and F. S. Navarra, “Double vector meson production in photon-hadron interactions at hadronic colliders,” Eur. Phys. J. C **76** (2016) no.7, 388 [arXiv:1605.05840 [hep-ph]].
- [44] G. Yang, J. Ping and J. Segovia, “Bottomonium-like tetraquarks in a chiral quark model,” [arXiv:2204.08556 [hep-ph]].
- [45] L. V. Gribov, E. M. Levin and M. G. Ryskin, “Semihard processes in QCD,” Phys. Rep. **100** (1983) 1.
- [46] L. D. McLerran and R. Venugopalan, Phys. Rev. D **49**, 2233 (1994) [hep-ph/9309289].
- [47] L. D. McLerran and R. Venugopalan, Phys. Rev. D **49**, 3352 (1994) [hep-ph/9311205].
- [48] L. D. McLerran and R. Venugopalan, Phys. Rev. D **50**, 2225 (1994) [hep-ph/9402335].
- [49] A. H. Mueller and J. Qiu, Nucl. Phys. B **268** (1986) 427
- [50] L. McLerran and R. Venugopalan, “Gluon distribution functions for very large nuclei at small transverse momentum,” Phys. Rev. D **49** (1994) 3352; “Green’s function in the color field of a large nucleus” **D50** (1994) 2225; “Fock space distributions, structure functions, higher twists, and small x ”, **D59** (1999) 09400.
- [51] K. J. Golec-Biernat and M. Wusthoff, Phys. Rev. D **60**, 114023 (1999) [hep-ph/9903358].
- [52] B. Z. Kopeliovich and A. V. Tarasov, Nucl. Phys. A **710**, 180 (2002) [hep-ph/0205151].
- [53] B. Kopeliovich, A. Tarasov and J. Hufner, Nucl. Phys. A **696**, 669 (2001) [hep-ph/0104256].
- [54] Y. V. Kovchegov, “Small x $F(2)$ structure function of a nucleus including multiple pomeron exchanges,” Phys. Rev. D **60** (1999), 034008 [arXiv:hep-ph/9901281 [hep-ph]].
- [55] Y. V. Kovchegov and H. Weigert, “Triumvirate of Running Couplings in Small- x Evolution,” Nucl. Phys. A **784** (2007), 188-226 [arXiv:hep-ph/0609090 [hep-ph]].
- [56] I. Balitsky and G. A. Chirilli, “Next-to-leading order evolution of color dipoles,” Phys. Rev. D **77** (2008), 014019 [arXiv:0710.4330 [hep-ph]].
- [57] Y. V. Kovchegov and E. Levin, “Quantum chromodynamics at high energy,” Camb. Monogr. Part. Phys. Nucl. Phys. Cosmol. **33** (2012), 1-350
- [58] I. Balitsky, “Effective field theory for the small x evolution,” Phys. Lett. B **518** (2001), 235-242 [arXiv:hep-ph/0105334 [hep-ph]].
- [59] F. Cougoulic and Y. V. Kovchegov, “Helicity-dependent generalization of the JIMWLK evolution,” Phys. Rev. D **100** (2019) no.11, 114020 [arXiv:1910.04268 [hep-ph]].
- [60] C. A. Aidala, *et al.*, “Probing Nucleons and Nuclei in High Energy Collisions,” [arXiv:2002.12333 [hep-ph]].

- [61] Y. Q. Ma and R. Venugopalan, “*Comprehensive Description of J/ψ Production in Proton-Proton Collisions at Collider Energies*,” Phys. Rev. Lett. **113** (2014) no.19, 192301 [arXiv:1408.4075 [hep-ph]].
- [62] V. M. Budnev, I. F. Ginzburg, G. V. Meledin and V. G. Serbo, “*The Two photon particle production mechanism. Physical problems. Applications. Equivalent photon approximation*,” Phys. Rept. **15** (1975), 181-281.
- [63] H. Kowalski and D. Teaney, Phys. Rev. D **68**, 114005 (2003) [hep-ph/0304189].
- [64] H. Kowalski, L. Motyka and G. Watt, Phys. Rev. D **74**, 074016 (2006) [hep-ph/0606272].
- [65] A. H. Rezaeian, M. Siddikov, M. Van de Klundert and R. Venugopalan, Phys. Rev. D **87**, no. 3, 034002 (2013) [arXiv:1212.2974 [hep-ph]].
- [66] S. Andrade, M. Siddikov and I. Schmidt, “*Exclusive photoproduction of heavy quarkonia pairs*,” Phys. Rev. D **105** (2022) no.7, 076022, [arXiv:2202.03288 [hep-ph]].
- [67] H. G. Dosch, T. Gousset, G. Kulzinger and H. J. Pirner, “*Vector meson leptoproduction and nonperturbative gluon fluctuations in QCD*,” Phys. Rev. D **55** (1997), 2602-2615 [arXiv:hep-ph/9608203 [hep-ph]].
- [68] J. Nemchik, N. N. Nikolaev and B. G. Zakharov, Phys. Lett. B **341**, 228 (1994); J. Nemchik, N. N. Nikolaev, E. Predazzi and B. G. Zakharov, Z. Phys. C **75**, 71 (1997); J. R. Forshaw, R. Sandapen and G. Shaw, Phys. Rev. D **69**, 094013 (2004).
- [69] E. Eichten, K. Gottfried, T. Kinoshita, K. D. Lane and T. M. Yan, Phys. Rev. D **17** (1978) 3090 Erratum: [Phys. Rev. D **21** (1980) 313].
- [70] E. Eichten, K. Gottfried, T. Kinoshita, K. D. Lane and T. M. Yan, Phys. Rev. D **21** (1980) 203.
- [71] C. Quigg and J. L. Rosner, Phys. Lett. **71B** (1977) 153.
- [72] A. Martin, Phys. Lett. **93B** (1980) 338.
- [73] S.J. Brodsky, T. Huang, G.P. Lepage, Proceedings of the Banff Summer Institute on Particles and Fields, held at the Banff Center in Banff, Alberta, Canada, August 16-27, 1981. Published as a standalone “Particles and Fields”, edited by A.Z. Capri and A.N. Kamal (Plenum Publishing Corporation, New York, 1983). DOI: 10.1007/978-1-4613-3593-1 , ISBN: 978-1-4613-3595-5
- [74] S. J. Brodsky, J. R. Hiller, D. S. Hwang and V. A. Karmanov, “*The Covariant structure of light front wave functions and the behavior of hadronic form-factors*,” Phys. Rev. D **69** (2004), 076001 [arXiv:hep-ph/0311218 [hep-ph]].
- [75] M. V. Terentev, “*On the Structure of Wave Functions of Mesons as Bound States of Relativistic Quarks*,” Sov. J. Nucl. Phys. **24** (1976), 106 ITEP-5-1976.
- [76] A. Stadler, S. Leitão, M. T. Peña and E. P. Biernat, “*Heavy and heavy-light mesons in the Covariant Spectator Theory*,” Few Body Syst. **59** (2018) no.3, 32 doi:10.1007/s00601-018-1355-1 [arXiv:1803.00519 [hep-ph]].
- [77] D. Daniel, R. Gupta and D. G. Richards, “*A Calculation of the pion’s quark distribution amplitude in lattice QCD with dynamical fermions*,” Phys. Rev. D **43** (1991), 3715-3724.
- [78] T. Kawanai and S. Sasaki, Phys. Rev. Lett. **107** (2011), 091601 [arXiv:1102.3246 [hep-lat]].
- [79] T. Kawanai and S. Sasaki, Phys. Rev. D **89** (2014) no.5, 054507 [arXiv:1311.1253 [hep-lat]].
- [80] A. H. Rezaeian and I. Schmidt, Phys. Rev. D **88** (2013) 074016, [arXiv:1307.0825 [hep-ph]].
- [81] H. Mäntysaari, N. Mueller and B. Schenke, “*Diffraction Dijet Production and Wigner Distributions from the Color Glass Condensate*,” Phys. Rev. D **99** (2019) no.7, 074004 [arXiv:1902.05087 [hep-ph]].
- [82] Y. Hatta, B. W. Xiao, F. Yuan and J. Zhou, “*Anisotropy in Dijet Production in Exclusive and Inclusive Processes*,” Phys. Rev. Lett. **126** (2021) no.14, 142001 [arXiv:2010.10774 [hep-ph]].
- [83] S. J. Brodsky, H. C. Pauli and S. S. Pinsky, “*Quantum chromodynamics and other field theories on the light cone*,” Phys. Rept. **301** (1998), 299-486 [arXiv:hep-ph/9705477 [hep-ph]].
- [84] J. D. Bjorken, J. B. Kogut and D. E. Soper, “*Quantum Electrodynamics at Infinite Momentum: Scattering from an External Field*,” Phys. Rev. D **3** (1971), 1382.